ChemComm
Chemical Communications

Accepted Manuscript

This article can be cited before page numbers have been issued, to do this please use: Z. Liu, T. Yu, D. Wei, Z. Li, L. Pan, Z. Zhang and Z. Tian, *Chem. Commun.*, 2020, DOI: 10.1039/C9CC09220J.

ROYAL SOCIETY OF CHEMISTRY

rsc.li/chemcomm

View Article Online
DOI: 10.1039/C9CC09220J

COMMUNICATION

Target-modulated sensitization of upconversionluminescence by NIR-emissive quantum dots: anew strategy to construct upconversionbiosensor

Received 00th January 20xx,
Accepted 00th January 20xx

DOI: 10.1039/x0xx00000x

Tianyu Yu,‡ Dong-Mei Wei,‡ Zhen Li, Liang-Jun Pan, Zhi-Ling Zhang, Zhi-Quan Tian*and Zhihong Liu*

We herein used Ag_2Se quantum dots (QDs) as a target-modulated sensitizer for upconversion nanoparticles (UCNPs) and the target thrombin as the sensitizing switch to construct a biosensor, circumventing the limited luminescence resonance energy transfer (LRET) efficiency of UCNPs, with enhanced signal-to-background ratio (SBR) and assay sensitivity.

Upconversion nanoparticles (UCNPs) can continuously absorb two or more low-energy photons to emit a single high-energy photon, which makes them excitable in the NIR region with reduced autofluorescence and scattering light in bioassays.[1-3] The nature of anti-Stokes emission endows UCNPs with the remarkable ability to avoid co-excitation of other luminescent materials, hence UCNPs are suitable energy donor in luminescence resonance energy transfer (LRET)-based assays.[4,5] Indeed, a majority of UCNPs-based sensors and probes are constructed with the LRET principle, in which organic dyes and nanomaterials, such as gold nanomaterials, carbon nanomaterials and two-dimensional covalent-network nanomaterials, are used as energy acceptors.[6-13] In these LRET-based sensing processes, the energy donors and acceptors are firstly brought to close proximity to trigger the energy transfer and quench the upconversion luminescence (UCL) of UCNPs. In the presence of sensing targets, the UCL can be restored because of the blocking of the LRET process induced by targets. In this way, the sensor/probe provides an “off-on” signal, and the signal-to-background ration (SBR) is principally determined by the LRET efficiency which is generally presented as the quenching efficiency of UCL.

As known, the LRET efficiency is highly dependent on the distance between energy donor and acceptor. Due to the rather large size of currently used UCNPs (usually larger than 20 nm),[14] only the emitting ions near the surface of the nanoparticles are quenchable by external energy acceptors, while those inner emitting ions doped in the matrix are non-quenchable and thus generate strong background signal.[15] Although the use of some nanosized energy acceptors can bring higher luminescence quenching efficiency due to the dipole-surface effect, there still exists a ceiling of UCL quenching efficiency which is currently being reported at around 90%. Besides, those nanosized energy acceptors may suffer from nonspecific adsorption which restricts the recovery of UCL after the recognition of targets.[12,13,16] Because of the above reasons, the SBR of upconversion nanoprobes and sensors normally fades next to those LRET-based counterparts with small-molecule luminophores as energy donors. Therefore, it is now in keen demand to find new strategies to construct upconversion probes/sensors so as to facilitate the application of upconversion luminescence in bioassay.

Dye-sensitization has recently been proposed to enhance UCL owing to the higher light absorption of dyes than lanthanide ions.[17,18] The dyes can absorb energy of photons and transfer their excited-state energy to UCNPs via a nonradiative energy transfer process. In our recent work, we built an upconversion nanoprobe using a NIR dye as the target-modulated sensitizing switch, which afforded a significantly improved SBR of ~30-fold.[19] In this system, the dye functioned as both the recognition unit of target and a potential antenna of UCNPs. After reacting with the target, the dye displayed a strong emission which overlaps with the absorption of UCNPs, resulting in the sensitization of UCL. This work has suggested the promising prospect of employing the dye-sensitization principle to conduct upconversion assays, which can be free of the limitation of energy-transfer efficiency from UCNPs to whatever energy acceptors. Nevertheless, the use of a proper NIR dye as sensitizer could be rather tricky because of the low quantum yield and small Stokes shift of most NIR dyes. The poor water solubility of NIR dyes is another concern increasing the difficulty in bioassays. Under such a circumstance, we pay our attention to quantum dots (QDs), seeking to use QDs as the potential sensitizer for UCNPs.

QDs are characterized with excellent photophysical properties and good chemical stability. They possess high quantum yield, large Stokes shift and adjustable emission peak with size change.[20,21] Quite a few kinds of QDs emitting in the NIR region have been reported, fulfilling the prerequisite of

Key Laboratory of Analytical Chemistry for Biology and Medicine (Ministry of Education), College of Chemistry and Molecular Sciences, Wuhan University, Wuhan 430072, China E-mail: zhhliu@whu.edu.cn
†Electronic Supplementary Information (ESI) available: Materials, methods, characterization and supplementary data. See DOI: 10.1039/x0xx00000x
‡ These authors contributed equally.

spectral overlap with the absorption of lanthanide ions. Herein, we propose a new strategy to fabricate upconversion biosensor based on direct enhancement of UCL by QDs (Scheme 1), with thrombin as the proof-of-concept target, which is an important biomarker playing great roles in life processes.[22] Ag_2Se QDs with intense emission around 980 nm was chosen as the energy donor and sensitizer to match the absorption of Yb^{3+}. Thus, Ag_2Se QDs are able to harvest the energy from excitation light and transfer their excited-state energy to Yb^{3+} ions via a nonradiative energy transfer process, given that they are brought to close proximity by the target thrombin. To avoid the interaction between these two kinds of nanoparticles and facilitate the subsequent biological modification, both of them were functionalized with carboxyl group. Two thrombin aptamers, namely TBA1 and TBA2, were covalently linked on the surface of UCNPs and Ag_2Se QDs through the amino group modified by the end of the DNA, respectively. The introduction of thrombin will simultaneously bind to these two aptamers and form thrombin-aptamers complex, shortening the distance between Ag_2Se QDs and UCNPs and triggering the energy transfer. As a consequence, the UCL of UCNPs will be enhanced depending on the concentration of thrombin.

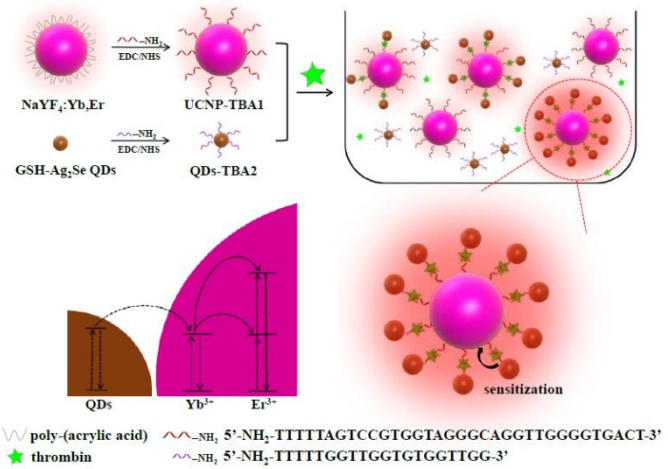

Scheme 1.Working principle of the thrombin sensor based on the target-modulated enhancement of UCL by Ag_2Se quantum dots

To realize the above design, the UCNPs with Yb^{3+} as the sensitizer and Er^{3+} as the emitter were selected as the energy acceptor. The obtained UCNPs were fairly uniform spheres with an average diameter of 24.4 nm (Fig.S1a-b, ESI†). The X-ray diffraction (XRD) peaks were consistent with standard β-$NaYF_4$ (Fig.S1c, ESI†), indicating the UCNPs nanocrystals were dominant in hexagonal phase. In order to improve the water solubility and facilitate the subsequent biological modification, PAA was utilized to replace the oleate ligands and stabilize UCNPs by coordination between the carboxyl groups and lanthanide ions on the surface of UCNPs. To expose the lanthanide ions, the oleate ligands were removed through acid treatment to obtain the bared UCNPs. Fourier transform infrared (FT-IR) analysis was employed to confirm not only the successful removal of oleic acid from UCNPs, but also the modification of PAA (Fig.S1d, ESI†). The aptamer TBA1 was covalently coupled on the surface of PAA-UCNPs by the reaction between the –COOH of PAA and the $-NH_2$ of TBA1. The conjugated product UCNPs-TBA1 exhibited an obvious absorption peak at 260 nm (Fig.S1e, ESI†), which was consistent with the typical absorption peak of DNA, verifying the successful biological connection between PAA-UCNPs and TBA1. More evidence of the functionalization by TBA1 can be found from zeta-potential measurement, which changed from -7.14 mV (PAA-UCNPs) to -12.6 mV (UCNPs-TBA1, Fig.S2, ESI†). According to the luminescence and absorption intensity of UCNPs-TBA1, the amount of TBA1 on each UCNP was estimated to be 17 copies(Fig.S3, ESI†).

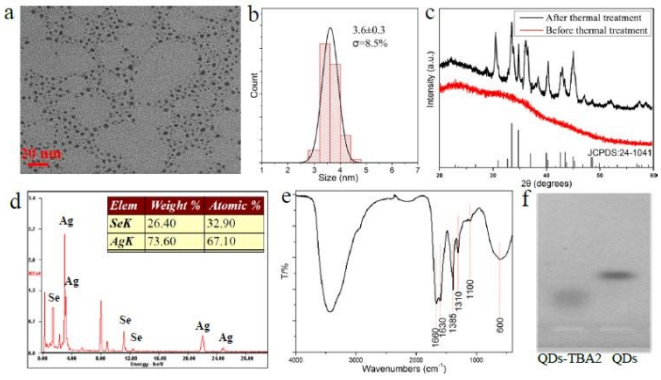

Fig.1 (a) TEM image, (b) Corresponding size distribution histogram, (c) XRD pattern, (d) EDX spectra and (e) FT-IR spectra of the as-prepared GSH-Ag_2Se QDs. (f) 1% agarose gel electrophoresis of QDs-TBA2 (on the left) and QDs (on the right), which was run at 130 V/cm for 15 min.

GSH stabilized Ag_2Se QDs were prepared by a one-pot synthesis method. The TEM image exhibited the GSH-Ag_2Se QDs were spheres of 3.6±0.3 nm in diameter with good dispersibility in aqueous solution (Fig.1a-b). The diffraction peaks of the as-prepared Ag_2Se QDs appeared after the thermal treatment, which matched well with the standard monoclinic Ag_2Se (JCPDS 24-1041) in XRD pattern (Fig.1c), indicating the products were indeed Ag_2Se nanocrystals. Energy dispersive X-ray (EDX) analysis verified the existence of Ag and Se elements in the Ag_2Se nanocrystals with the appropriate stoichiometry of bulk Ag_2Se (Fig.1d). GSH stabilized the Ag_2Se QDs through the Ag-S covalent bonds, and the carboxyl groups of GSH could be used to conjugate with biomolecules containing amino groups. In the FT-IR spectra (Fig.1e), the absorption peaks at 1600 cm^{-1} and 1385 cm^{-1} were assigned to the asymmetric and symmetric C=O stretching vibration, the peak at 1660 cm^{-1} was the vibration peak of the amide C=O in GSH, the peak at 600 cm^{-1} was the out-of-plane deformation vibration of N-H in secondary amide of GSH, the peak at 1310 cm^{-1} was the vibration peak of methylene in GSH, and the peak at 1100 cm^{-1} was the stretching vibration peak of C-N in amine of GSH. Lastly, there was no absorption peak at 2490 cm^{-1} assigned to the free sulfhydryl group, indicating the successful conjugation between the -SH group of GSH and Ag_2Se QDs. The obtained Ag_2Se QDs displayed a distinct absorption before 1100 nm and an obvious emission around 980 nm, which well matched with the absorption of Yb^{3+}, ensuring the effective energy transfer from the Ag_2Se QDs to Yb^{3+} (Fig.S4, ESI†). Then, the aptamer TBA2 was modified on the surface of the QDs through the amino bond. The 1%

agarose gel electrophoresis experiment was performed to ensure the successful conjugation of TBA2 and GSH-Ag_2Se QDs (Fig.1f). The band of QDs was ahead of QDs-TBA2 conjugates due to the larger molecular weight of QDs-TBA2 conjugates than that of QDs, making the conjugates move relatively slower under the same voltage. Furthermore, the zeta-potential of QDs and QDs-TBA2 were -34.3 mV and -42.7 mV, respectively, which further verified the successful connection of QDs and the aptamer (Fig.S5, ESI†). The number of TBA2 on each QD was estimated to be 5 copies (Fig.S6, ESI†).

Before the detection of thrombin, a series of experimental conditions were optimized to endow the biosensor with the best performance. In all of the following experiments, the concentration of UCNP-TBA1 was fixed at 0.05 mg/mL. At first, we investigated the optimal ratio of QDs to TBA2 in the conjugation experiment. The quantity of QDs was fixed at 5 nmol, and different amounts of TBA2 were utilized to conjugate with QDs. When the amount of TBA2 was 2 nmol (Fig. S7, ESI†), the UCL enhancement factor reached the maximum, which was not further improved with increasing the amount of TBA2. Thus, the amount of TBA2 for conjugation was determined as 2 nmol per 5 nmol QDs in follow-up experiments. Meanwhile, the concentration of QDs-TBA2 conjugate displayed a great impact on the experimental results.

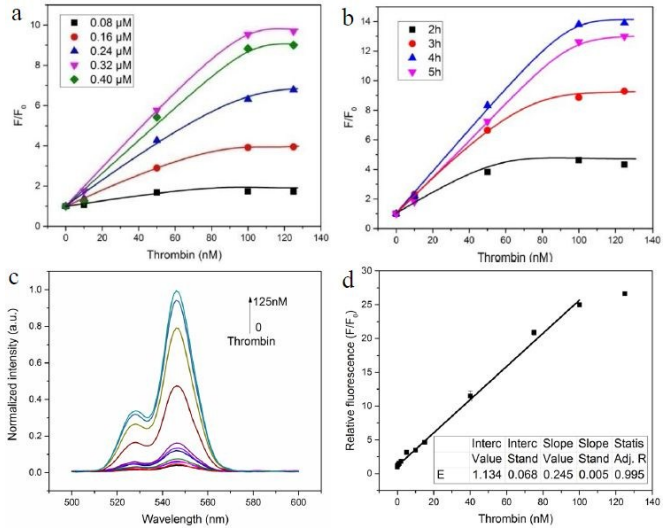

Fig.2 The UCL enhancement factors (F/F_0, in which the F and F_0 represent the UCL intensity in the presence and absence of thrombin) of biosensor responding to different concentration of thrombin under different conditions: (a) various amounts of QDs-TBA2, and (b) different reaction time. (c) UCL emission spectra of the biosensor in aqueous buffer, and (d) the linear relationship between the UCL enhancement factor and the concentration of thrombin in the range from 0.1 nM to 125 nM.

Although the QDs-TBA2 with higher concentration could enhance the absorption of excitation light to improve the UCL enhancement factor, the excess QDs-TBA2 would quench the emission of UCNPs because of the inner filter effect. Thus, we explored the suitable concentration of QDs-TBA2 was 0.32 μM (Fig.2a), with which the highest signal-to-background was achieved. Furthermore, we found that the UCL enhancement factors depended on the incubation time. As shown in Fig.2b, in the suitable concentration of QDs-TBA2, the optimal incubation time was 4 h.

After acquiring the optimal conditions for assay, we then investigated the performance of this biosensor for thrombin detection in aqueous buffer. With the addition of thrombin in the mixture containing the fixed concentration of UCNPs-TBA1 and QDs-TBA2, the UCNPs and QDs were taken into close proximity through the formation of thrombin-aptamers complex, leading to the effective energy transfer from QDs to UCNPs and the enhanced UCL emission. As shown in Fig.2c, the UCL enhancement factor, i.e., the SBR defined above, was linearly related to the concentration of thrombin in the range of 0.1-100 nM. To our delight, a maximum UCL enhancement factor of ~27 was achieved under the optimal conditions with the thrombin concentration of 125 nM (Fig.2d). Notably, such a SBR is much higher than that of the majority of existing upconversion sensors based on “off-on” signals. The limit of detection (LOD) was calculated to be 0.034 nM on the basis of $3S_b/k$ criterion, where k is the slope of the linearity in the detection range and S_b is the standard deviation of blank (n = 7). Compared with other thrombin biosensors based on UC-LRET principle, our method presented a direct UCL enhancing strategy without the limitation of LRET efficiency and offered a relatively lower LOD and wider linear range (Table S1, ESI†). Furthermore, in order to preclude possible effect of thrombin itself on UCL intensity, different concentrations of thrombin were incubated with UCNPs-TBA1 for 4 h. No significant change of UCL intensity was detected (Fig.S8, ESI†). The energy transfer efficiency from QDs to UCNPs was calculated as 20%, according to the fluorescence intensities of QDs in the mixture of UCNPs-TBA1 and QDs-TBA2 in the absence and presence of thrombin (Fig.S9, ESI†). To point out, this is not a high energy-transfer efficiency, suggesting that there still has a plenty room to further improve the energy-transfer rate from QDs to UCNPs as well as the SBR in the future. The thrombin induced assembly of UCNPs-TBA1 and QDs-TBA2 was also evidenced by TEM images (Fig.S10, ESI†). Although the QDs showed low contrast in the images, we can see that QDs were randomly scattered around the UCNPs before the addition of thrombin; while in the presence of thrombin the QDs gathered around the UCNPs. All the above results elucidated that the target-mediated sensitization of UCL by QDs can provide a simple and straightforward yet highly sensitive assay for thrombin.

Before applying this biosensor in complex biological sample matrix, the specificity was firstly studied by incubating UCNPs-TBA1 and QDs-TBA2 mixture with thrombin and several other biological species in aqueous buffer. As observed, none of these substances gave rise to obvious fluorescence alteration except thrombin (Fig.S11, ESI†). This result indicated the pronounced specificity of the proposed biosensor for thrombin and could be competent in complex biological samples.

To estimate the feasibility of using this biosensor in complex sample matrix, it was applied in a series of human serum samples with different dilution folds, which was diluted with HEPES buffer to keep the pH at 7.4. Although the UCL enhancement factors were reduced with decreasing the dilution folds (Fig. S12, ESI†) probably due to the existence of abundant interferences impeding the assembly of QDs with

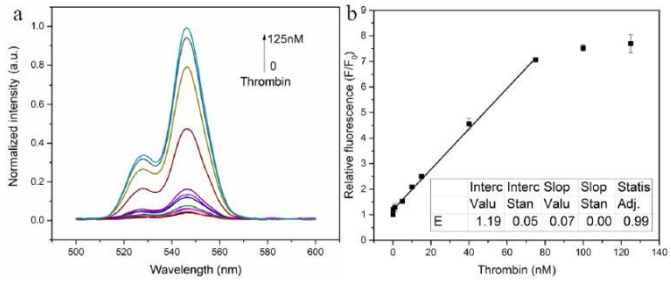

Fig.3(a) Upconversion luminescence spectra of the biosensor in 100-fold diluted serum sample, and (b) the linear relationship between F/F_0 and the concentration of thrombin within the range of 0.1 nM-125 nM. F_0 and F represent luminescence intensity in the absence and presence of thrombin.

UCNPs and restricting the energy transfer, the similar thrombin concentration-dependent UCL enhancement as that in aqueous buffer was still detected. In a 100-fold diluted human serum, a SBR of 7.0 was obtained (Fig.3a), and a linear range for thrombin from 0.1 nM to 75 nM was also achieved (Fig.3b) with a LOD of 0.091 nM ($3S_b/k$ criterion). Furthermore, standard addition experiments were conducted in 100-fold diluted serum sample with the recoveries in the range from 91.93% to 102.8% and RSD from 0.749% to 6.97% (Table S2, ESI†), implying this biosensor still works in complex samples.

The practical applicability of this biosensor was ultimately studied by detecting the levels of thrombin in plasma samples. As known, thrombin exists in its precursor form, prothrombin, in blood plasma. Therefore, 7 human plasma samples from healthy volunteers obtained from the university hospital were first pretreated with 0.03 M $CaCl_2$ to convert prothrombin into thrombin, followed by the same assay procedure as in serum. The results obtained by our method were in good agreement with the results from commercial ELISA kit (Table S3, ESI†). The values of t_{exp} based on t-test statistical analysis were less than that of t_{crit} ($t_{crit[0.05,4]}$= 2.78) in all the seven cases. Therefore, the accuracy of our biosensor was acceptable for thrombin detection in real clinical samples. In order to verify the universality of our strategy, we separately tagged two aptamers of carcinoembryonic antigen (CEA) onto UCNPs and QDs for the detection of CEA. With a similar assay protocol, the UCL enhancement factor was linearly related to the concentration of CEA in the range of 0.1-20 ng/mL and a maximum UCL enhancement factor of ~19-fold with a LOD of 0.045ng/mL ($3S_b/k$ criterion) was achieved (Fig.S13, ESI†).

In summary, we developed a new strategy to construct UCNPs-based biosensors through target-modulated direct UCL enhancement by a QDs-sensitization process. This strategy not only achieved significantly higher SBR than traditional LRET-based upconversion biosensors, but also simplified the operation as compared to the traditional "off-on" biosensors. The new biosensor provided good performance in both buffered solutions and diluted serum samples for thrombin. A 27-fold SBR was achieved in the aqueous solution, which is significantly higher than that of most LRET-based upconversion sensors. More significantly, the sensor displayed high accuracy in real clinical samples. This is a simple yet highly effective strategy for the construction of upconversion biosensors, which could be readily extended to other analytes through simply adopting other recognition modes (like nucleic acid hybridization, immunoreaction or other aptamers), suggesting a promising prospect in biomedical study and clinical diagnosis.

Conflicts of interest

There are no conflicts to declare.

Acknowledgements

This work was financially supported by the National Natural Science Foundation of China (Grant No. 21575109, 21625503) and Major Projects of Technical Innovation of Hubei Province (No. 2017ACA172).

Notes and references

1 Z. Li, S. W. Lv, Y. L. Wang, S. Y. Chen and Z. H. Liu, *J. Am. Chem. Soc.* 2015, **137**, 3421-3427.
2 G. Y. Chen, H. L. Qiu, P. N. Prasad and X. Y. *Chen, Chem. Rev.* 2014, **114**, 5161-5214.
3 X. J. Zhu, Q. Q. Su, W. Feng and F. Y. Li, *Chem. Soc. Rev.* 2017, **46**, 1025-1039.
4 Q. Q. Su, W. Feng, D. P. Yang and F. Y. Li, *Acc. Chem. Res.* 2017, **50**, 32-40.
5 T. Y. Sun, F. J. Ai, G. Y. Zhu and F. Wang, *Chem. Asian J.* 2018, **13**, 373-385.
6 M. Y. He, Z. Li, Y. Y. Ge and Z. H. Liu, *Anal. Chem.* 2016, **88**, 1530-1534.
7 X. S. Chen, J. M. Lan, Y. X. Liu, L. Li, L. Yan, Y. K. Xia, F. Wu, C. Y. Li, S. R. Li and J. H. Chen, *Biosens. Bioelectron.* 2018, **102**, 582-588.
8 W. Ma, P. Fu, M. Z. Sun, L. G. Xu, H. Kuang and C. L. Xu, *J. Am. Chem. Soc.* 2017, **139**, 11752-11759.
9 K. Y. Zhang, L. Yang, F. Lu, X. C. Wu and J. J. Zhu, *Small* 2018, **14**, 1703858.
10 R. R. Deng, X. J. Xie, M. Vendrell, Y. T. Chang and X. G. Liu, *J. Am. Chem. Soc.* 2011, **133**, 20168-20171.
11 J. Yuan, Y. Cen, X. J. Kong, S. Wu, C. L. Liu, R. Q. Yu and X. Chu, *ACS Appl. Mater. Interfaces* 2015, **7**, 10548-10555.
12 C. L. Zhang, Y. X. Yuan, S. M. Zhang, Y. H. Wang and Z. H. Liu, *Angew. Chem. Int. Ed.* 2011, **50**, 6851-6854.
13 H. Rabie, Y. X. Zhang, N. Pasquale, M. J. Lagos and P. E. Batson, *Adv. Mater.* 2019, **31**, 1806991.
14 Z. H. Li, H. Yuan, W. Yuan, Q. Q. Su and F. Y. Li, *Coord. Chem. Rev.* 2018, **354**, 155-168.
15 Z. M. Zhang, S. Shikha, J. L. Liu, J. Zhang, Q. S. Mei and Y. Zhang, *Anal. Chem.* 2019, **91**, 548-568.
16 Y. H. Wang, L. Bao, Z. H. Liu and D. W. Pang, *Anal. Chem.* 2011, **83**, 8130-8137.
17 W. Q. Zou, C. Visser, J. A. Maduro, M. S. Pshenichnikov and J. C. Hummelen, *Nat. Photonics* 2012, **6**, 560-564.
18 X. D. Wang, R. R. Valiev, T. Y. Ohulchanskyy, H. Ågren, C. H. Yang and G. Y. Chen, *Chem. Soc. Rev.* 2017, **46**, 4150-4167.
19 T. Liang, Z. Li, P. P. Wang, F. Z. Zhao, J. Z. Liu and Z. H. Liu, *J. Am. Chem. Soc.* 2018, **140**, 14696-14703.
20 N. Hildebrandt, C. M. Spillmann, W. R. Algar, T. Pons, M. H. Stewart, E. Oh, K. Susumu, S. A. Díaz, J. B. Delehanty and I. L. Medintz, *Chem. Rev.* 2017, **117**, 536-711.
21 J. Chang, Y. Liu, J. Li, S. L. Wu, W. B. Niu and S. F. Zhang, *J. Mater. Chem. C* 2013, **1**, 1168-1173.
22 B. L. Li, Y. L. Wang, H. Wei and S. J. Dong, *Biosens. Bioelectron.* 2008, **23**, 965-970.